

## MICROMEGAS TPC R&D

P. COLAS, I. GIOMATARIS, J. MARTIN, A. OLIVIER, Ph. REBOURGEARD  
*DSM/Dapnia, CEA/Saclay, F-91191 Gif sur Yvette CEDEX, France*

J. JEANJEAN, V. LEPELTIER  
*LAL Orsay, F-91405 Orsay, France*

M. RONAN  
*LBNL, Berkeley, CA 94720, USA*

Studies of the properties and performances of small gap wire chambers and Micromegas detectors for LC-TPC readout are presented. Gas amplification, drift and attachment studies, and aging effects are reported for Micromegas devices with several different gases and mixtures. Preliminary results on positive ion feedback in a 2 T magnetic field are summarized. The design of a small Micromegas TPC prototype with fine metallic micromesh structures of different pitches and anode pad readout for testing in a high magnetic field is discussed.

### 1 Introduction

Large Time Projection Chamber (TPC) detectors are being designed for a future Linear Collider (LC). These next generation TPC detectors will have full pad coverage to provide excellent overall pattern recognition and tracking. Conventional TPC's using wires for electron multiplication have large cathode pad response corrections and  $E \times B$  effects. TPC R&D on new Micro-Pattern Gas Detectors (MPGD) which provide gas electron amplification within microstructures is being performed to obtain better resolution and to allow finer readout segmentation. In October 2001, the DESY Physics Research Committee (PRC), recommended the approval of the LC TPC program<sup>5</sup>, and : *“encourages the collaboration to perform in High magnetic fields tests of the different end-plate geometries (GEM, Micromegas, and the standard wire chambers)....* The work described here intends to fulfill part of this goal, namely the micromegas and wire chamber studies.

The advantages of Micromegas for reading out a TPC are listed in Section 2. In Section 3 we report on the various tests and measurements carried out to assess the feasibility of a micromegas TPC, and in Sections 4 and 5 we describe the measurement of the feedback in the magnetic field respectively for a wire chamber TPC and a micromegas TPC. In Section 6 we report on the prototype under construction by the Berkeley-Orsay-Saclay collaboration for a cosmic ray test in a magnetic field in Saclay.

## 2 Principle and advantages of MICROMEGAS

In a micromegas detector, a 3 to 5  $\mu\text{m}$  thick mesh divides the gas volume in two parts: a low-field – typically 200 V/cm – ‘drift’ region and a high-field – 40-70 kV/cm ‘amplification’ region, typically 50-100 micron thick.

A Micromegas TPC is a Micromegas detector (MICRO-MESH GASEOUS detector)<sup>1</sup> where the conversion and drift region extends over a large distance, allowing the coordinate along the drift field to be measured through the drift time of the charge bucket. Equivalently, a Micromegas TPC is a standard TPC where the wire chamber has been replaced by a Micromegas device. There is a slight difference between these two schemes as far as readout electronics is concerned: whereas the electron signal on the pads is positive (it is the image charge of the avalanche which takes place on the wires), it is negative in the case of Micromegas, where the avalanche takes place very close to the pads.

Micropattern Gaseous Detector TPCs which use GEMs<sup>2</sup> or Micromegas readout planes offer several advantages with respect to standard wire TPCs. They appear more and more to be a necessary improvement of the TPC techniques in view of its application to the Linear Collider. First of all, in a wire chamber, the electric field is radial near the wires, generating a spread of the electron cluster of more than hundred microns by  $E \times B$  effect along the wire direction. In a micropattern detector, the region where the field is not parallel to the magnetic field is much reduced. Also, due to the high density of tracks in the jets produced at high energy and due to the high background, a high granularity and an excellent 2-track resolution (a few millimeters) are required. For instance, for a 250 GeV  $\tau$  jet in 3 prongs, the tracks are not separated by more than 8 mm. Clearly the 3 to 5 cm pads used in LEP detectors would be too large for disentangling neighbouring tracks at the LC. Micropattern detectors allow a much more granular pad structure.

Micromegas presents advantages over other micropattern detectors. The gain shows a maximum as a function of the gap for a given voltage applied. In standard conditions of operation, this optimal gap is a few tens of microns<sup>3</sup>. This makes the gain independent of the gap, to first order, and gives a good potential for  $dE/dx$  resolution, provided that the gap and the gas composition can be matched to an optimum. Micromegas has also proved to be usable with a gas mixture containing  $\text{CF}_4$  as a quencher. Such a hydrogen-less gas would respond much less to the neutron backgrounds than isobutane, methane, and other hydrocarbons. Such a ‘neutron-tolerant’ gas cannot be used without efficiency loss in structures where fields of the order of a few kV/cm exist over a mm or so, as is the case in wire chambers and GEMs. Indeed, the electron spectrum overlaps the attachment resonance for such fields. Another advantage

of Micromegas for a TPC is the natural ion feedback suppression it provides, thanks to the funnel effect studied in Sections 3, 4, and 5. In Micromegas the fast ion signal (about 50 ns) does not suffer from ballistic deficit : it is entirely transmitted through a fast charge amplifier that allows operation at quite a low gain (less than 1000 for the Linear Collider TPC). In a MWPC, because of the ballistic deficit, and in GEM because of partial transmission of the electrons, the loss can be as high as an order of magnitude, which has to be compensated by an operation at higher gain, and thereby more ion feedback. Micromegas detectors are easy to build, and as large as  $40 \times 40 \text{ cm}^2$  have functionned. Last but not least, Micromegas are successfully used in two large experiments at CERN (COMPASS<sup>4</sup> and NA48), breaking records of rate and time resolution for gaseous detectors.

### 3 Study of various properties of a Micromegas TPC

A number of experiments have been conducted to perform studies of various aspects of a LC TPC. The drift velocity of electrons has been measured in several gases using a laser to produce photoelectrons from two grids distant by a few millimeters: the mesh and the drift cathode. The method and the results of the measurements have been described elsewhere<sup>6</sup>. Argon-CF<sub>4</sub> mixtures have been shown to have a maximum velocity of up to  $7 \text{ cm}/\mu\text{s}$  at fields as low as  $200 \text{ V/cm}$ . Simulations, supported by our measurements, show that there is no attachment for fields below  $400 \text{ V/cm}$ . An aging test has been performed using this gas, with a X-ray gun. A total of  $2 \text{ mC/mm}^2$ , well above the requirements for a linear collider, have been accumulated without decrease of the signal.

Extensive studies have been carried out of the ion feedback. In a Micromegas TPC, the electric field ratio between the amplification field (40 to 70 kV/cm) and the drift field (typically  $200 \text{ V/cm}$ ) is usually high (about 300). Under such conditions, most of the field lines originating at the anode end at the micromesh. As the diffusion is negligible for ions, the ions produced on these field lines do not go back to the drift volume and most of them will be neutralised on the mesh. If the extension of the avalanche is not too large compared to the hole pitch the ion feedback is optimal, and equal to the inverse of the field ratio. This is called the ‘funnel effect’.

#### 4 Study of the ion feedback in a small-gap wire chamber TPC in a magnetic field

Classical wire chamber TPCs have been operated for years at various  $e^+e^-$  colliders in magnetic fields up to 1.5 tesla. To be a backup solution for the LC TPC, such a device must have small enough distances between the sense wires, and between the wire plane and the pads, so that the influence of the charge created near a wire is limited to a small number of narrow pads. We thus built a *small gap* wire chamber,  $10 \times 10 \text{ cm}^2$ , where the  $20 \mu\text{m}$  diameter sense wires, at a high positive potential, sitted 2 mm from the pads. Its pitch was 1.5 mm. A grounded wire grid at 2 mm from the sense wire plane separated the drift volume from the detection volume. The conversion and drift space was 10 mm thick. The drift electrode was set to a negative potential of typically 250 V, but was varied from 100 V to 1000 V.

The primary ionisation was provided by a 25 MBq  $^{55}\text{Fe}$  source. The gas used was Ar:CH<sub>4</sub> 90:10, except in a first measurement with zero magnetic field where Ar-isobutane was used. The sense wires were kept at a potential of 2000 V in the first measurement and 2080 V in the others. The gain in the chamber was of the order of  $10^4$ .

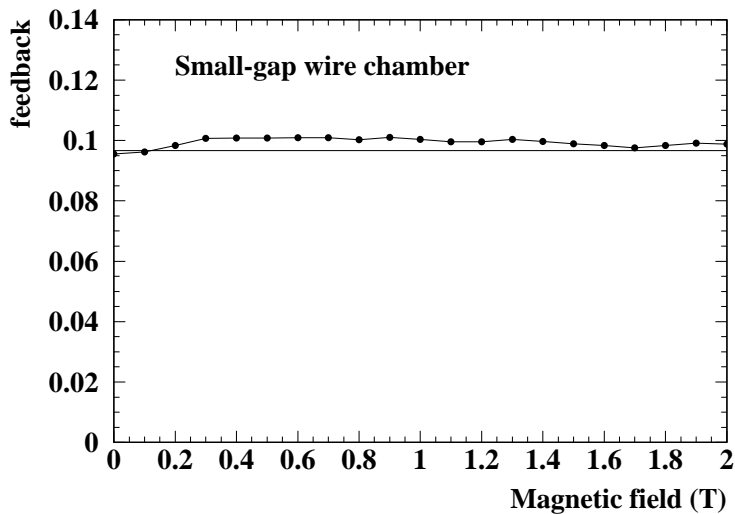


Figure 1: Positive ion feedback *vs.* magnetic field for the small-gap wire chamber TPC.

The currents in the  $i_{wire}$  and  $i_{drift}$  in the wire and the drift power supplies were monitored, allowing the measurement of the positive ion feedback  $f$  from the relation  $f = (i_{drift} - i_0)/i_{wire}$ , where  $i_0$  is the primary ionisation, measured to be about 5.3 nA in conditions where the voltage on the wires was lowered to 1400 V to work in the ionisation chamber mode *i.e.* with no gain. The currents in this experiment ranged typically from a few nA to 150 nA. A small correction is applied to the voltages as the current goes through a 100 M $\Omega$  resistor, part of a T-filter for the noise. This correction ranges from less than 1 V to 15 V for the sense wire voltage. The feedback is shown as a function of the magnetic field in Fig 1.

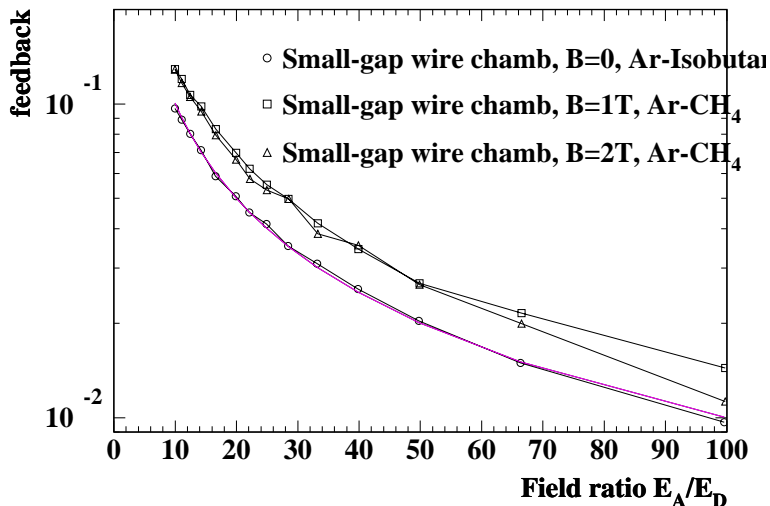


Figure 2: Positive ion feedback *vs.* ratio of amplification to drift electric fields for the small-gap wire chamber TPC. Data are shown for three values of the magnetic field : 0, 1 and 2 tesla. The lower curve shows the ideal case were the feedback is equal to the inverse of the field ratio. Note that the data taken with no magnetic field were taken with an Argon-isobutane (90:10) mixture.

An effective electric field ratio can be defined as the ratio of the average field in the cell ( $V_{wires}/2$  mm) to the drift field. The dependance of the measured feedback on this effective electric field ratio is shown in Fig 2. For three values of the magnetic field. The data at B=0 were taken with an Argon-isobutane (90:10) mixture, whereas the data at B=1 T and 2 T used

an Argon-methane (90:10) mixture. The inverse-field ratio law is well obeyed for Ar-isobutane and an increase of 20% on the feedback is observed for Ar-methane, as expected from a lower diffusion in this gas.

## 5 Study of the feedback in a micromegas TPC in a magnetic field

We have built a small TPC with a 1 cm drift length and a micromegas. The mesh pitch is 500 lines per inch and the gap is  $50 \mu\text{m}$ . The grid is in copper, as preliminary tests in the magnet showed that nickel grids are deformed by the magnetic field.

The primary ionisation was provided by a 1 GBq  $^{60}\text{Sr}$  source. The gas used was Ar:CH<sub>4</sub> 90:10. The gain in the chamber was measured to be up to 3300 (Fig 3). The  $^{60}\text{Sr}$  nucleid emits a 2 MeV  $\beta$  ray and the primary

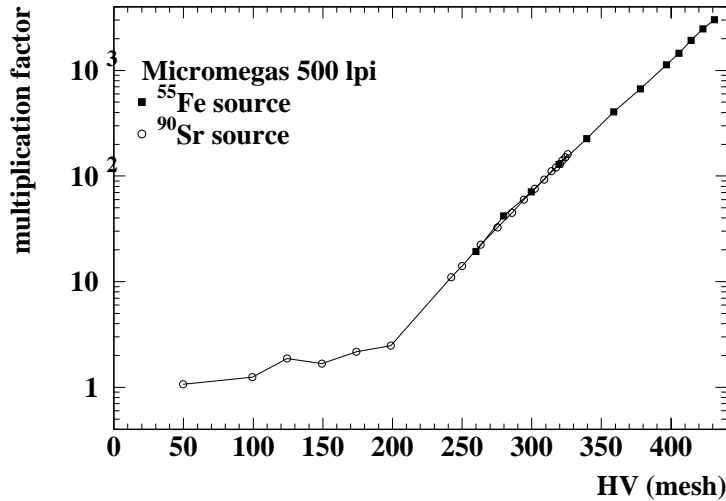


Figure 3: Current driven through the mesh (arbitrary units) as a function of the voltage applied on the mesh.

ionisation is thus dependent on the magnetic field, as the path length and the acceptance of the detector depends on it. The data are corrected to take into account this effect, which cancels out in the feedback measurement. The positive ion feedback  $f$  is obtained from the supply currents by the relation  $f = (i_{drift} - i_0)/(i_{wire} + i_{drift})$ , where  $i_0$  is the primary ionisation. The

measured feedback is shown as a function of the magnetic field in Fig 4. The line is the expectation from the inverse electric-field ratio law. It is not flat as, due to the combined effect of the resistors mentioned in previous section and the dependance of the primary ionisation on the magnetic field, the field ratio depends on the magnetic field. In these measurements, the drift field was 300 V/cm and the amplification voltage was 340 V, which corresponds to a gain of 350. These conditions are close to the operating conditions at a linear collider.

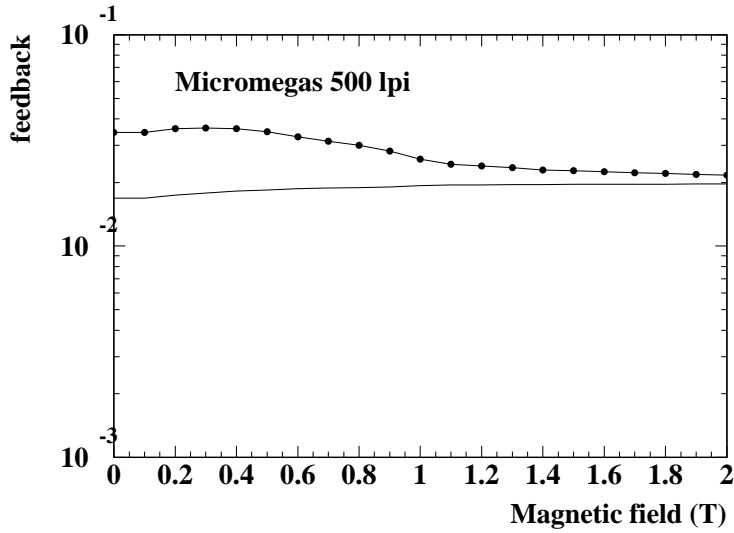


Figure 4: Positive ion feedback vs magnetic field for the micromegas TPC.

The positive ion feedback is shown in Fig 5 as a function of the field ratio. The departure by a factor of 4 with respect to the ideal case (inverse field ratio) is consistent with the expectation of 3.2, given the uncertainties on the gap and on the gas parameters. This factor of 3.2 is due to the relatively coarse grid used in these measurements (50 micron pitch, whereas the optimum of 1 could be reached for a 25 micron pitch).

In conclusion, the operation of a micromegas TPC in a magnetic field has been demonstrated. The feedback does not depend significantly on the magnetic field and the expected feedback suppression factors of a few per mil should be obtained in ideal conditions.

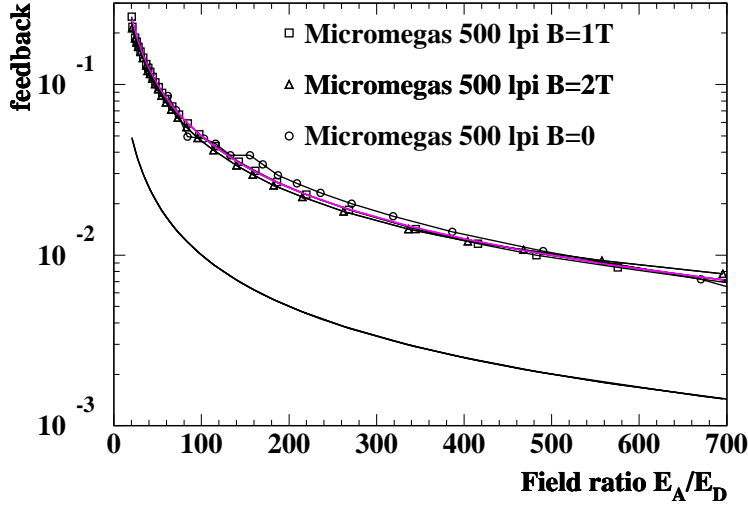


Figure 5: Positive ion feedback *vs.* ratio of amplification to drift electric fields for the micromegas TPC. Data are shown for three values of the magnetic field : 0, 1 and 2 tesla. The lower curve shows the ideal case were the feedback is equal to the inverse of the field ratio.

## 6 The cosmic ray prototype

A large micromegas TPC prototype (50 cm drift length, 53 cm diameter) is under construction (see Fig 6). It is fitted to the bore of the 2 tesla superconducting magnet RMN 530, a medical NMR magnet recently brought back to operation in Saclay after 12 years of use in the Orsay hospital. The magnetic field is homogeneous within 1% over the drift area. The electric field is provided by a cylindrical field cage 40 cm in diameter, made of a series of circular copper rings interconnected through resistors to provide an homogeneous electric field. The Very High Voltage supply is recuperated from the DELPHI TPC at LEP and will provide an electric drift field up to 400 V/cm. The cage has been designed to allow for a laser beam and a radioactive source to be used for test purposes. The micromegas endplate is removable, allowing to test various pad configurations, and to study possible improvements as for instance a resistive layer to improve the sharing of the signal on several pads<sup>7</sup>. It can also be replaced by a wire chamber, still considered as a backup solution for the



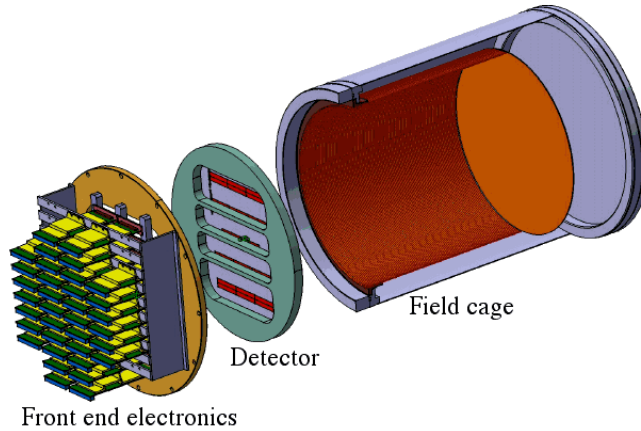


Figure 6: Cosmic ray TPC setup.

LC TPC. In the baseline version of the setup, the PC board of the endplate wears 50 micron high and 200 micron diameter polyimide pillars, positionned every millimeter, used as spacers to support the micromesh. The 500 lpi copper micromesh has been manufactured at the CERN workshop. The PC board carries anode pads arranged in 10 lines: 8 lines of 96 ( $2 \text{ mm} \times 10 \text{ mm}$ ) pads, and 2 lines of 128 ( $1 \text{ mm} \times 10 \text{ mm}$ ) pads. The readout pads are connected through the PC boards by metallized vias. On the external side of the PC board, connectors are soldered by short wires. The front end readout cards (a total of 1152 channels) are recuperated from the STAR TPC at RHIC, and have been modified to allow for the amplification, sampling and digitization of negative signals as those provided by a micromegas TPC.

The trigger is provided by a coincidence of two layers of scintillators placed below and above the magnet.

The first tests of this setup are scheduled for the spring of 2003.

## Acknowledgments

We would like to thank the Saclay Magnet and Cryogenics department (SACM) for having operated the 2T magnet successfully. We also wish to thank the engineers and technicians for their help in designing and building the cosmic ray prototype and mounting the magnet experiment: F. Bieser, R. Cizeron, P. Desaunais, E. Delagnes, A. Giganon, G. Guilhem and P. Imbert.

## References

1. I. Giomataris *et al.*, *Nucl. Instrum. Methods* A376 (1996) 29.
2. F. Sauli, *Nucl. Instrum. Methods* A386 (1997) 531.
3. G. Charpak *et al.*, *Nucl. Instrum. Methods* A478 (2002) 26.
4. A. Magnon *et al.*, *Nucl. Instrum. Methods* A478 (2002) 210.
5. R. Settles *et al.* LC TPC R and D, DESY PRC 01-03 (October 2001).
6. P. Colas *et al.*, *Nucl. Instrum. Methods* A478 (2002) 215.
7. K. Sachs, these proceedings.